



UNIVERSITÀ  
DEGLI STUDI  
FIRENZE

# FLORE

## Repository istituzionale dell'Università degli Studi di Firenze

### **Characterization of airborne particulate matter in an industrial district near Florence by PIXE and PESA**

Questa è la Versione finale referata (Post print/Accepted manuscript) della seguente pubblicazione:

*Original Citation:*

Characterization of airborne particulate matter in an industrial district near Florence by PIXE and PESA / M. CHIARI; F. LUCARELLI; F. MAZZEI; S. NAVA; L. PAPERETTI; P. PRATI; G. VALLI; R. VECCHI. - In: X-RAY SPECTROMETRY. - ISSN 0049-8246. - ELETTRONICO. - 34:(2005), pp. 323-329. [10.1002/xrs.825]

*Availability:*

This version is available at: 2158/212293 since: 2017-10-16T16:35:20Z

*Publisher:*

John Wiley & Sons Limited:1 Oldlands Way, Bognor Regis, P022 9SA United Kingdom:011 44 1243 779777,

*Published version:*

DOI: 10.1002/xrs.825

*Terms of use:*

Open Access

La pubblicazione è resa disponibile sotto le norme e i termini della licenza di deposito, secondo quanto stabilito dalla Policy per l'accesso aperto dell'Università degli Studi di Firenze (<https://www.sba.unifi.it/upload/policy-oa-2016-1.pdf>)

*Publisher copyright claim:*

(Article begins on next page)

# Characterization of airborne particulate matter in an industrial district near Florence by PIXE and PESA<sup>†</sup>

M. Chiari,<sup>1</sup> F. Lucarelli,<sup>1\*</sup> F. Mazzei,<sup>2</sup> S. Nava,<sup>1</sup> L. Paperetti,<sup>1</sup> P. Prati,<sup>2</sup> G. Valli<sup>3</sup> and R. Vecchi<sup>3</sup>

<sup>1</sup> Department of Physics and INFN Florence, via Sansone 1, I-50019 Sesto Fiorentino, Italy

<sup>2</sup> Department of Physics and INFN Genoa, via Dodecaneso 33, I-16146 Genoa, Italy

<sup>3</sup> Institute of Applied General Physics and INFN Milan, via Celoria 16, I-20133 Milan, Italy

Received 10 September 2004; Accepted 5 January 2005

The composition of airborne particulate matter in Montelupo Fiorentino (a small town about 20 km west of Florence characterized by the presence of a large number of ceramic and glass factories) was studied by means of continuous and sequential sampling, ion beam analysis (IBA) techniques and statistical methods. The aerosol PM<sub>10</sub> fraction was collected on a daily basis for about 9 months (September 2002–June 2003). To investigate the elemental size distribution, for a shorter period (about 3 weeks) we collected PM<sub>10</sub>, PM<sub>2.5</sub> and PM<sub>1</sub> simultaneously. A continuous streaker sampler was also used, which allows the study of the aerosol composition with 2 h time resolution. Mass concentrations were obtained using an analytical balance. The elemental analysis was performed at the INFN accelerator laboratory at the Physics Department of Florence University by particle-induced x-ray emission and particle elastic scattering analysis (the latter implemented for this campaign). The use of the two techniques allowed a complete reconstruction of the gravimetric mass. An absolute principal component analysis showed industrial sources to be, on average, the main contributors to PM<sub>10</sub> mass; however, the weight of the 'soil' source (connected to local soil re-suspension and to long-range Saharan transport episodes) becomes dominant during some of the days when the 50  $\mu\text{g m}^{-3}$  limit is exceeded. Copyright © 2005 John Wiley & Sons, Ltd.

## INTRODUCTION

Montelupo Fiorentino is a small town (10 000 inhabitants) about 20 km west of Florence, characterized by the presence of a large number of factories, mainly producing ceramics, glassware and terracottas, and also related activities such as a paint factory. According to the regulations in force, the total suspended PM<sub>10</sub> particulate mass is monitored by the local authority. Since the PM<sub>10</sub> mean value in the area is higher than the current Italian Air Quality Directive (DM60/2002) recommended value and potentially harmful elements can be emitted by the local industrial activities, we decided to start an extensive investigation, whose purposes were (1) to determine PM<sub>10</sub> concentration and composition [by particle-induced x-ray-emission (PIXE)], collecting samples for a long period; (2) to determine, for a certain period, the mass concentrations and the elemental composition also of the PM<sub>1</sub> and PM<sub>2.5</sub> fractions of the aerosol; (3) to determine by particle elastic scattering analysis (PESA) the concentrations of H, C, N and O, which are important contributors to the aerosol, allowing a complete reconstruction of the mass; and

(4) to identify the major pollution sources and their impact, using also a streaker sampler with 2 h time resolution.

## EXPERIMENTAL

### Aerosol sampling

The particulate matter samples were collected on 47 mm diameter Teflon (CF<sub>2</sub>) filters by three sequential particle samplers on a daily basis. The first, the Partisol 2025, is designed for a flow-rate of 1 m<sup>3</sup> h<sup>-1</sup> and may be equipped with the EPA-standard PM<sub>10</sub> and PM<sub>2.5</sub> inlets; it can also collect PM<sub>1</sub> using a WINS impactor (located before the filter). The others are two IND PNS15D sequential particulate samplers, which work at a higher flow-rate (2.3 m<sup>3</sup> h<sup>-1</sup>) and may be equipped with PM<sub>10</sub> (CEN EN 12341 reference sampler), PM<sub>2.5</sub> and PM<sub>1</sub> inlets. The samplers were located 4 m above ground level, on the roof of an air quality monitoring station, keeping the three inlets at a distance of about 2 m from each other, to avoid any interference of their air flows. The sampling campaign started on 24 September 2002 and ended on 24 June 2003. In the first part of the campaign (until 30 October) we used the three samplers with the same inlet (PM<sub>10</sub> or PM<sub>2.5</sub> or PM<sub>1</sub>, 10 days for each size fraction) to carry out a systematic comparison between the concentrations measured by the three devices; from 1 to 21 November we put a different inlet on each instrument to measure the size fraction ratios (i.e. PM<sub>1</sub> to PM<sub>2.5</sub> and PM<sub>2.5</sub> to PM<sub>10</sub>). Starting from 23 November, we continued the sampling with only one IND sampler with a PM<sub>10</sub> inlet.

\*Correspondence to: F. Lucarelli, Department of Physics and INFN Florence, via Sansone 1, I-50019 Sesto Fiorentino, Italy.

E-mail: lucarelli@fi.infn.it

<sup>†</sup>Presented at 10th International Conference on Particle Induced X-ray Emission and its Analytical Applications, PIXE 2004, Portoroz, Slovenia, 4–8 June 2004.

Contract/grant sponsor: Italian Ministry of Education, University and Research; Contract/grant number: COFIN2001.

Owing to some technical problems during the campaign, we obtained PM<sub>10</sub> samples for about 200 days and PM<sub>2.5</sub> and PM<sub>1</sub> samples for about 30 days.

From 13 February until 12 March, we also collected the fine and coarse fractions of the aerosol with a 2 h time resolution by a streaker sampler. The sampling device is a commercial two-stage streaker made by PIXE International (Tallahassee, FL, USA). It is designed to separate, at a flow-rate of about 1 l min<sup>-1</sup>, the fine (aerodynamic diameter <2.5 µm) and the coarse (2.5–10 µm) modes of the aerosol. A pre-impactor stops particles with diameter >10 µm. A paraffin-coated 7.5 µm thick Kapton (C<sub>22</sub>H<sub>10</sub>N<sub>2</sub>O<sub>5</sub>) foil is used as an impaction surface for coarse particles and a 0.4 µm pore-size Nuclepore (C<sub>15</sub>H<sub>14</sub>CO<sub>3</sub>) filter as a fine particle collector. A control unit ensures a steady air flow through the streaker.<sup>1</sup> The impaction plate and the filter are paired on a circular cartridge, which rotates in front of a pumping orifice of ~1.2 mm width, in our study at a constant angular speed of about 2° every 2 h (i.e. a shift equal to the orifice width); on the impaction plate and the filter a sampling of 2 weeks is carried out.

The PM<sub>10</sub>, PM<sub>2.5</sub> and PM<sub>1</sub> daily mass concentrations were obtained by weighing the filters before and after the sampling, always after a storage period (48 h) in a temperature- and humidity-controlled room (ambient temperature = 20 ± 1 °C, relative humidity = 50 ± 5%), by an analytical balance (sensitivity 1 µg); electrostatic effects are avoided by the use of a deionizing gun.

### PIXE analysis

The concentrations of the elements with  $Z > 10$  were measured by PIXE at the external beam facility of the KN3000 3 MV Van de Graaff accelerator in Florence.<sup>2</sup> Typically, in aerosol measurements a 3 MeV proton beam is extracted in air through an Upilex window of 7.5 µm thickness. The particulate matter samples are positioned at a distance of about 1 cm from the window, perpendicular to the beam; taking into account the energy loss in the extraction window and in the path in atmosphere, the final proton energy on the target is about 2.85 MeV. The beam size is determined by bare collimation under vacuum in the last section of the beamline. PIXE analysis of aerosol samples with an external beam is preferable for several reasons: it facilitates handling, positioning, changing and/or scanning of the samples; it assures good heat dissipation, thus drastically reducing the risk of selective loss of some aerosol components under beam irradiation (especially Cl and Br, which are the most volatile); the problem of local heating is much smaller, especially when using a helium flow, which is a very efficient heat remover; mechanical stresses, which occur during the transient between ambient and high vacuum, are avoided; and electrical charging of insulated target (like aerosol samples) does not occur.

Since x-ray production cross-sections range over three orders of magnitude, to obtain an efficient simultaneous detection of all the elements it is necessary to balance the counting rates produced by the low- and medium-high- $Z$  elements. The adopted solution is the use of a fairly high beam current (5–15 nA) and two Si(Li) detectors (Si1 and

Si2 in the following), optimized for low and medium-high x-ray energies, respectively. Si1 (13 mm<sup>2</sup> area, 3 mm thick, 170 eV resolution) is placed at about 145° relative to the beam direction, at a distance of about 6 cm from the target. Thanks to the ultra-thin entrance window (8 µm of Be) and to the use of a helium gas flow into the volume in front of the detector, Si1 can detect with good efficiency x-rays of very low energies, down to ~1 keV (Na K $\alpha$  line). Moreover, the He flux drastically reduces in the PIXE spectra the height of the Ar peak from the residual air. Since low-energy x-ray production cross-sections are higher (and also low- $Z$  elements are generally the most abundant in aerosol samples), Si1 is collimated to 3 mm<sup>2</sup>. Si2 (80 mm<sup>2</sup> area, 5 mm thick, 190 eV resolution) is placed at 135°, at a distance of about 2–3 cm from the target. A Mylar foil of about 400 µm is used to attenuate the low-energy x-rays. The beam charge is integrated by a graphite Faraday cup placed behind the sample.

A common problem in all PIXE set-ups is the backscattering of protons from the target that damages the detector and perturbs the electronic system, increasing the pile-up very significantly and deteriorating the energy resolution. In our facility, this problem arises only for Si1, since its Be window and the helium flow in front of detector allow the backscattered protons to reach the detector itself, whereas Si2 is shielded by the Mylar absorber in front of its entrance window. To prevent protons from reaching Si1 without employing any shielding material, which would absorb also the low-energy x-rays, we mounted in front of the detector a proton deflector placed at <1 cm from the active volume of the detector. An Nd-Fe-B permanent magnet machined as a parallelepiped (1.5 × 1.5 × 4 cm) was small enough to be mounted parallel to the short path from the sample to the detector. The magnetic field (0.5 T) was strong enough to deflect backscattered protons with energies up to 3 MeV. We observed that, using the proton deflector, in the worst situation (i.e. analysis of the streaker samples on Kapton and Nuclepore substrates), we achieved a halving of the pile-up and an enhancement of the energy resolution.

Two different set-ups, the 'daily sample set-up' and the 'streaker sample set-up', allow easy handling, positioning, changing and scanning of samples collected by sequential samplers and streaker samplers, respectively. To make the analysis of daily samples automatic, in order to exploit the intrinsic speed of the PIXE technique and to analyse a large number of samples in a short period, we used a multi-target holder, which manages the changing and scanning of 32 filters. The deposit area is about 12 cm<sup>2</sup> and has to be scanned by the beam, to average out possible inhomogeneities. During irradiation (about 10 min per sample, with a beam current ranging from 5 to 10 nA), the filters were moved in front of the beam so that most of the area of deposit was analysed. The streak produced by the streaker sampler is analysed 'point by point' using a beam size which corresponds to 2 h of aerosol sampling. To have a uniform distribution of the beam current intensity over the probed area, the beam is defocused under vacuum by means of magnetic quadrupoles and then, before the extraction window, collimated to a rectangular spot (1 × 3 mm), corresponding to 2 h of aerosol sampling on the

Kapton foil. On Nuclepore filters, on which the streak vertical size is 8 mm, the  $1 \times 3$  mm beam is moved vertically along the streak to average out possible deposition inhomogeneities. One 'point' is irradiated for about 5 min at a current of 10–15 nA, then next 'point' is immediately exposed to the beam by simply moving the filter by a stepping motor, in automated sequences. Scanning the whole streaker requires about 15 h with, on average,  $3 \mu\text{C}$  collected per each step.

In the analysis of daily samples, the fluorine content of Teflon filters gave rise in the PIXE spectra to a strong Compton  $\gamma$ -ray background, owing to the high production rate of  $\gamma$ -rays, which worsened the PIXE detection limits for medium–high- $Z$  elements. Moreover, at currents above 6–7 nA, the pile-up in the Si2 detector reached unsustainable levels and saturation was reached in the preamplifier. To reduce the F-induced background, the proton beam energy was lowered, thus decreasing the  $\gamma$ -ray production cross-sections.<sup>3,4</sup> We made some tests at 2.2 MeV (energy on the target, corresponding to 2.4 MeV proton energy in vacuum), and we compared the results with spectra obtained at the usual working energy of 2.85 MeV: the background in the 10–30 keV energy range in the PIXE spectra decreased a factor of  $\sim 3$  and the resulting minimum detection limits (MDLs) for medium–high- $Z$  elements improved by a factor of  $>2$ . Furthermore, with a reduced beam energy, the Si2 pile-up rate can be maintained within acceptable levels (5%). Note that also the MDLs of Ti, V, Cr and Mn improved owing to the reduction of the maximum energy of the secondary bremsstrahlung background. Hence, all the PIXE measurements on daily samples were performed at 2.2 MeV proton energy (Fig. 1).

PIXE spectra were fitted using the GUPIX software package<sup>5</sup> and elemental concentrations were obtained via a calibration curve constructed using a set of thin standards

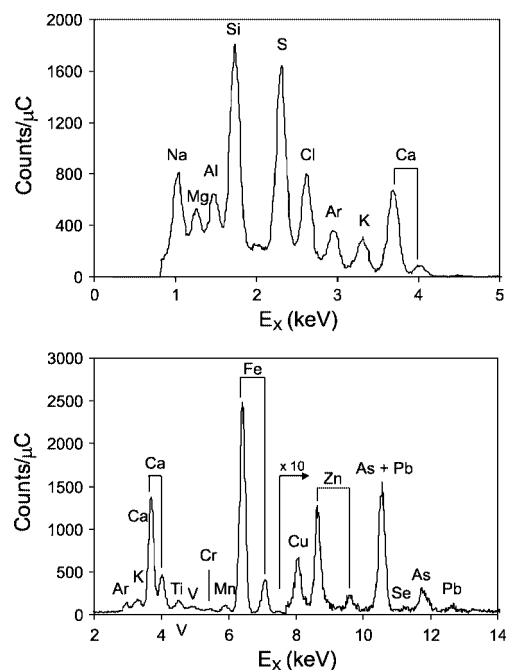


**Figure 1.** PIXE spectra of a PM<sub>10</sub> sample collected on a Teflon filter (Montelupo Fiorentino, 20 November 2002). Proton energy, 2.2 MeV; beam current, 6 nA.

of known areal density. A check of the overall accuracy of the experimental procedure was made by analysing the BCR 128 standard (Fly Ashes on Artificial Filter) from the Community Bureau of Reference and the NIST SRM 2783 standard (Air Particulate on Filter Media) from the National Institute of Standards and Technology. Both standards were moved in front of the beam, to average out possible inhomogeneities. The reproducibility was also checked by analysing the same aerosol samples over different measurement runs.

Elemental concentrations in air are deduced through the knowledge of the sampling parameters (area of the deposit, air flow-rate, duration of sampling). The associated uncertainty is determined by a sum of independent uncertainties on standard sample thickness (5%), peak areas (from 2 to 20% or higher when concentrations approach MDLs)—which include x-rays counting statistics, background subtraction and peak overlaps—and aerosol deposition area and sampler air flow (of the order of few percent).

Detection limits were about  $10 \text{ ng m}^{-3}$  for low- $Z$  elements and about  $1\text{--}2 \text{ ng m}^{-3}$  (or below) for medium–high- $Z$  elements. The following elements were looked for: Na, Mg, Al, Si, P, S, Cl, K, Ca, Ti, V, Cr, Mn, Fe, Ni, Cu, Zn, As, Se, Br, Sr, Zr, Cd, Sb, Ba and Pb.

Blank filters were also analysed in order to detect background elements; only Nuclepore filters showed Ca and Fe impurities whose concentrations exceeded their MDLs, remaining, however, much smaller than the contribution coming from the aerosol samples. Anyway, the blank contribution was always subtracted.

## PESA analysis

To obtain a complete reconstruction of the aerosol mass, we implemented the detection of H, C, N and O by in-vacuum PESA. The use of Teflon filters was mandatory for the application of this technique, since they were the only substratum appropriate among all the membranes commonly used in aerosol sampling in terms of beam irradiation resistance, absence of H, N and O and low C concentration in their composition. Note that for the last two reasons the collected streaker samples were not analysed by PESA.

Details of the experimental set-up and data analysis have been given elsewhere;<sup>6</sup> here some essential features are briefly recalled.

For the in-vacuum PESA measurements we worked with protons at an energy of 3 MeV; we used two fully depleted surface-barrier detectors of  $300 \mu\text{m}$  thickness,  $50 \text{ mm}^2$  area and about 20 keV energy resolution, arranged at forward and backward angles. The detector used to measure the H content was placed at a  $30^\circ$  scattering angle and collimated to  $0.8 \text{ mm}^2$ , whereas the other detector, used for the C, N and O concentration determinations, was placed at  $150^\circ$  and collimated to  $15 \text{ mm}^2$ ; both detectors were 65 mm apart from the sample, which was placed in a vertical plane orthogonal to the beam. The resulting acceptance solid angles allowed one to compensate roughly for differences in count rates at the different angles. The beam dimensions on the sample were  $2 \times 2 \text{ mm}$ . The beam current was integrated, after the sample, by a Faraday cup, kept at a positive voltage of about 70 V to avoid secondary electrons escape.

The contribution due to the carbon content of the filter to be subtracted from the total C signal is proportional to the 'local' filter thickness and, assuming a constant C/F ratio, to its F content, which can be measured by particle-induced  $\gamma$ -ray emission (PIGE) analysis (simultaneously with PESA), exploiting the  $^{19}\text{F}(p,p'\gamma)^{19}\text{F}$  reaction ( $E_\gamma = 110$  keV).

Quantitative results were obtained through a calibration achieved using a thin Upilex foil containing known areal densities of H, C, N and O, comparable to those found in aerosol samples.

The adopted method for C measurements was successfully checked using carbon black standards prepared depositing a powder of carbon black with known areal density (ranging from 20 to 180  $\mu\text{g cm}^{-2}$ ) on Teflon filters.

Typical MDLs were 0.3  $\mu\text{g cm}^{-2}$  for H, 4  $\mu\text{g cm}^{-2}$  for C and 2  $\mu\text{g cm}^{-2}$  for N and O. The absolute H concentration could be measured to within  $\pm 10\%$ , whereas for the other elements the uncertainty ranged from  $\pm 10$  to  $\pm 30\%$ , with the largest uncertainties affecting the N concentration.

Note that, owing to the longer time needed for the in-vacuum PESA measurements compared with PIXE, at present only half of the total daily samples collected have been analysed with this technique.

## RESULTS

### Sequential sampler comparison

The first part of the sampling campaign was devoted to verifying the equivalence of the three sequential samplers in terms of weighted mass and elemental concentrations. This comparison was mandatory since one of our goals was to determine the total mass and elemental size fraction ratios (i.e.  $\text{PM}_1$  to  $\text{PM}_{2.5}$  and  $\text{PM}_{2.5}$  to  $\text{PM}_{10}$ ) using the three devices simultaneously. Therefore, we used the three sequential samplers with the same inlet for 10 days for each size fraction ( $\text{PM}_{10}$ ,  $\text{PM}_{2.5}$  and  $\text{PM}_1$ ).

Concerning the aerosol mass concentration determined gravimetrically, the comparison was made following the CEN EN12341 Directive. This procedure refers only to  $\text{PM}_{10}$ ; however owing to the absence of any directive for  $\text{PM}_{2.5}$  and  $\text{PM}_1$ , we applied the same procedure to all the size fractions. The comparison showed very good agreement: the mass concentrations measured by the three devices differed by  $< 6 \mu\text{g m}^{-3}$  in the  $\text{PM}_{10}$  fraction and  $< 3 \mu\text{g m}^{-3}$  in the  $\text{PM}_{2.5}$  and  $\text{PM}_1$  fractions during all samplings. Moreover, the correlation coefficients of the concentration time trends measured by pairs of samplers were better than 0.98.

The elemental concentrations, obtained by PIXE and PESA, also turned out to be in agreement for all three fractions within the experimental uncertainties; as an example, in Fig. 2 the results obtained from the analysis of the  $\text{PM}_{10}$  samples collected on 4 October are shown.

### $\text{PM}_{10}$ characterization

The average value of  $\text{PM}_{10}$  concentration over the whole sampling period (180 days in total) was 32  $\mu\text{g m}^{-3}$  and on 21 days  $\text{PM}_{10}$  concentration was  $> 50 \mu\text{g m}^{-3}$ , a limit value not to be exceeded more than 35 times per year (EU Air Quality Directive EC/30/1999).

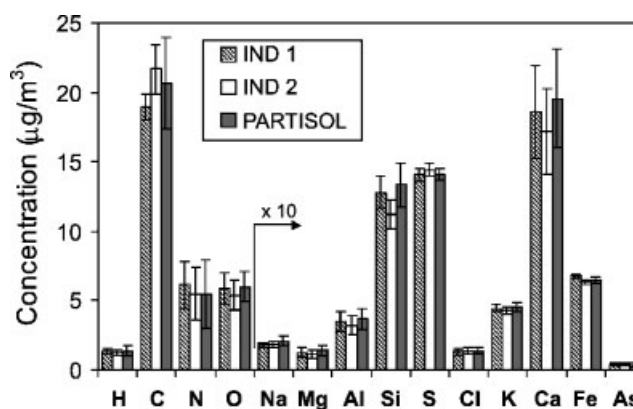


**Figure 2.** Elemental concentrations obtained from the analysis of  $\text{PM}_{10}$  samples collected on 4 October 2002 by three sequential samplers (two IND PNS15D and one Partisol 2025).

**Table 1.**  $\text{PM}_{10}$  mean elemental concentrations ( $\text{ng m}^{-3}$ ), calculated over the whole data set ( $\sim 200$  samples analysed by PIXE and  $\sim 100$  samples analysed by PESA)<sup>a</sup>

Element	$\text{ng m}^{-3}$	Element	$\text{ng m}^{-3}$
H	690	V	5
C	13 120	Cr	3
N	6300	Mn	14
O	3880	Fe	530
Na	270	Ni	4
Mg	130	Cu	14
Al	320	Zn	35
Si	980	As	10
P*	10	Se	4
S	950	Br	4
Cl	280	Sr*	6
K	340	Zr*	13
Ca	1440	Pb	19
Ti	35		

<sup>a</sup> Values were calculated using MDLs for the cases in which the element was not detected. Elements detected on  $< 50\%$  of the days are marked with an asterisk; for these the reported value should be considered as a conservative upper estimate.

The average concentrations of the detected elements in the  $\text{PM}_{10}$  fraction are reported in Table 1. Several species such as Ni, As and Pb are often classified as toxic, and their mean concentrations in Table 1 should be noted. The Pb concentration was well below the European exposure limits ( $0.5 \mu\text{g m}^{-3}$  yearly average of daily concentrations). The average As concentration is 10  $\text{ng m}^{-3}$ , higher than the future limit of 6  $\text{ng m}^{-3}$  (yearly average of daily concentrations). However, the concentration of this element, which, in Montelupo Fiorentino, is related to emissions from artistic glass manufactures, assumed very high values (with peaks up to 100  $\text{ng m}^{-3}$ ) during the first sampling months, but a sharp decrease was observed starting from December (Fig. 3), which was ascribed to changes in glass production activities (as confirmed by representatives of local industries). The average concentration of Ni was well below the future limit of 20  $\text{ng m}^{-3}$ .

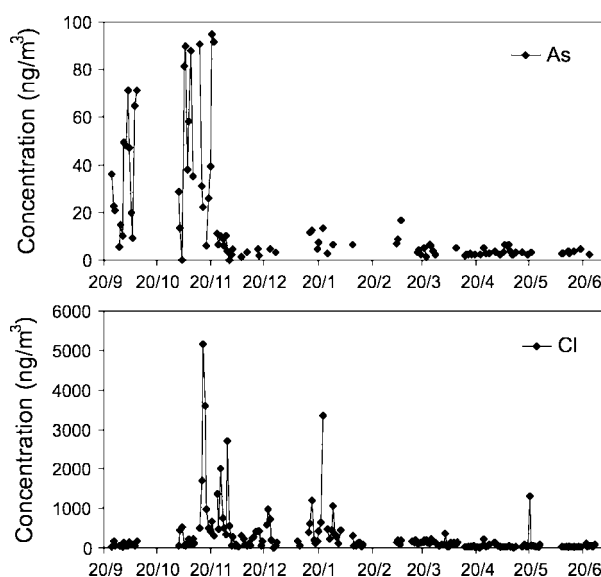


Figure 3. As and Cl daily concentrations in the PM<sub>10</sub> fraction.

The trend of Na and Cl is noteworthy, characterized by intense episodes over a lower background (in Fig. 3 the Cl time series is shown as an example): these episodes are typical of marine aerosol transported occasionally by wind. Backward trajectories ending in Montelupo Fiorentino during these days were calculated by the HYSPLIT transport model<sup>7</sup> (NOAA Air Resource Laboratory) on an hourly basis. For all these episodes we found trajectories coming from the Tyrrhenian Sea and characterized by high wind intensities (air masses still on the sea a few hours before approaching the sampling site), confirming the hypothesis of transported marine aerosol.

### Size distribution

The co-located sampling of the PM<sub>10</sub>, PM<sub>2.5</sub> and PM<sub>1</sub> (period 1–21 November 2002) allowed us to determine the division of the weighted mass and elemental concentrations into these three fractions.

Excluding three days during which there was an anomalous increase in PM<sub>10</sub> mass concentrations with respect to PM<sub>2.5</sub> and PM<sub>1</sub> (see below, Saharan dust intrusions), PM<sub>2.5</sub> and PM<sub>1</sub> turned out to be a substantial part of PM<sub>10</sub>; in particular, the average fraction ratios and their standard deviation were PM<sub>2.5</sub>/PM<sub>10</sub> = 0.60 ± 0.08 and PM<sub>1</sub>/PM<sub>10</sub> = 0.44 ± 0.07.

The elemental distributions are shown in Fig. 4. As expected, the elements more concentrated in the coarse

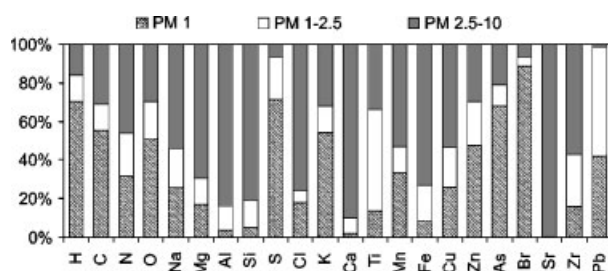


Figure 4. Percentage decomposition of the elemental concentrations in the three size fractions.

fraction are those of crustal origin (Al, Si, Ca, Fe, Sr); however, also Zr, which is produced by the manufacturing of tiles, is mainly present in the PM<sub>2.5–10</sub> fraction.

H, C, O, S, K, Zn, As, Br and Pb are mainly present in the PM<sub>2.5</sub> and PM<sub>1</sub> fractions. In particular, S is concentrated to >90% in the PM<sub>2.5</sub> fraction; in fact, this element is mainly produced in the atmosphere by heterogeneous reactions, which transform SO<sub>2</sub> (gas emitted from fossil fuel combustion processes) into sub-micrometric sulfate particles.

### Mass closure

PIXE–PESA measurements allowed a fairly good reconstruction of the gravimetric mass. The ratio between the sum of the concentrations of all the detected elements and the weighted mass, averaged over the ~100 samples of PM<sub>10</sub> analysed by both techniques, was 0.95 ± 0.10, with a correlation coefficient  $r = 0.96$ . The average contributions of PIXE and PESA to the reconstructed mass turned out to be 18 and 82%, respectively. As regards the ‘missing’ 5% of the reconstructed mass, that might hint at some small systematic errors (in PESA analysis) or the onset of selective volatilization of light elements under vacuum (e.g. nitrogen compounds).

In Fig. 5, the mean contributions of the eight most abundant elements detected by PIXE and PESA to the total PM<sub>10</sub> mass are shown: C (44%), N (20%) and O (12%) are the main aerosol components and, among PIXE elements, the more abundant ones are Ca, Si, S and Fe.

Considering elements of crustal origin as oxides (Na<sub>2</sub>O, MgO, SiO<sub>2</sub>, Al<sub>2</sub>O<sub>3</sub>, TiO<sub>2</sub>, K<sub>2</sub>O, CaO, Fe<sub>2</sub>O<sub>3</sub>), the mass of the ‘soil component’ was ~20% of the PM<sub>10</sub> mass. Following the hypothesis that all the sulfur can be ascribed to ammonium sulfate, the contribution of this compound is ~10%.

### Saharan dust intrusions

In southern Europe, a significant contribution to particulate matter mass is made by desert dust transported from North Africa. The dry climate and the scarcity of precipitation in the Mediterranean favour a long residence time of particles in the atmosphere with a consequent impact on PM<sub>10</sub> concentration levels.<sup>8</sup> Owing to the different health effects, it is important to distinguish between high concentration levels due to these natural episodes and those produced by pollution events. The EU Air Quality Directive EC/30/1999 sets the limit value for PM<sub>10</sub> as 40 µg m<sup>-3</sup> as an annual average and states

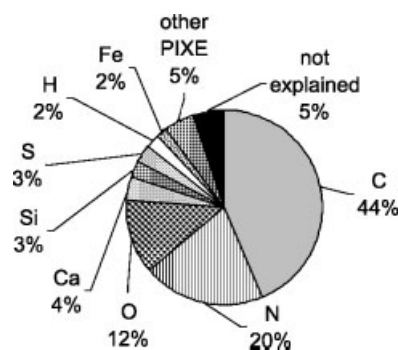
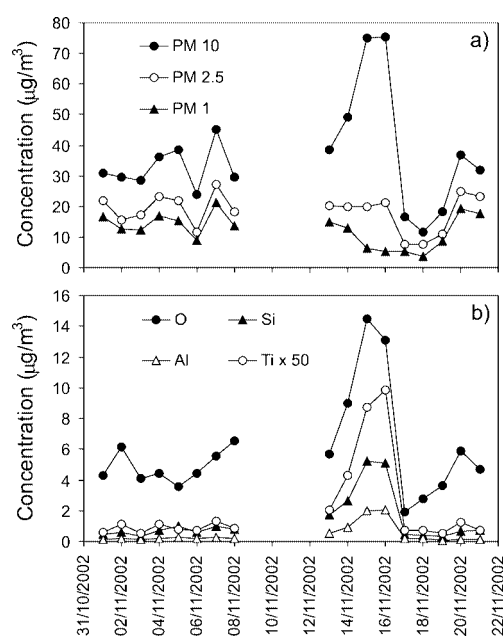


Figure 5. Average contributions (percentage) of the eight most abundant detected elements to the total PM<sub>10</sub> mass.

that the daily value of  $50 \mu\text{g m}^{-3}$  must not be exceeded more than 35 days per year. However, in order to focus on emissions strictly related to anthropogenic activity, the Directive specifies that these limits are not to be applied to events defined as natural (volcanic eruptions, geothermal and seismic activities, re-suspension of particles, long-range transport from arid zones, etc.).

Thanks to the granulometric size fractionation and to the multi-elemental feature of the PIXE and PESA techniques, during this campaign some Saharan dust intrusions were clearly identified; the strongest occurred on 14–16 November 2002, during the simultaneous sampling of the three fractions. This episode was characterized by a strong increase in the  $\text{PM}_{10}$  concentration (up to  $75 \mu\text{g m}^{-3}$ ), not followed by the  $\text{PM}_{2.5}$  and  $\text{PM}_1$  concentrations [Fig. 6(a)] and by an increase of all soil-related elements (e.g. Al, Si, Ca, Ti, Fe and O) in the  $\text{PM}_{10}$  fraction [examples are given in Fig. 6(b)]. The percentage of the  $\text{PM}_{10}$  mass explained by the 'soil component' during this episode was more than twice the average value over the whole sampling period. Furthermore a change in the concentration ratios for crustal elements was observed; in particular, Si/Fe, Al/Fe and Ti/Fe ratios assumed values which were twice their average values (Table 2) and closer to those expected for desert dusts.<sup>9</sup>



**Figure 6.** Daily concentrations of  $\text{PM}_{10}$ ,  $\text{PM}_{2.5}$  and  $\text{PM}_1$  (top panel), and of some soil-related elements in the  $\text{PM}_{10}$  fraction (bottom panel) during the Saharan dust intrusion and on the days immediately before and after.

**Table 2.** Element ratios during the Saharan dust episode with, for comparison, the average values calculated over the whole sampling period

Element ratio	Average value	15 November	16 November
Si/Fe	$1.8 \pm 0.4$	2.8	2.5
Al/Fe	$0.6 \pm 0.2$	1.1	1.0
Ti/Fe	$0.06 \pm 0.02$	0.09	0.10

Backward trajectory calculations (HYSPLIT transport model by NOAA Air Resource Laboratory) confirmed the hypothesis of the Saharan origin: air masses approaching the sampling site during these 3 days were above Libyan and Algerian deserts just 1–2 days before.

### APCA analysis

The identification of the sources is obviously one of the most important issues in particulate matter studies: it is necessary for any pollution abatement strategy. Multi-elemental techniques, such as IBA analyses, can be of great help, since aerosol particles retain elemental compositions characteristic of their origin, even at long distances, and the simultaneous detection of groups of elements may be a signature of the sources. Receptor models, such as principal component analysis (PCA), group the detected elements into 'factors' (or 'components') according to the similarity of the time behaviour of their concentrations, thus succeeding in identifying the sources of pollution.

Starting from the data obtained for  $\text{PM}_{10}$  for the whole sampling period, a PCA with Varimax rotation was carried out to identify the main aerosol sources. The elements which were below their MDL on >30% of sampling days were not included in the analysis. Other elements were below the MDL in a fewer instances: in those cases a random value between zero and the MDL was attributed to the element concentration.<sup>10</sup> Since only about half of the  $\text{PM}_{10}$  daily samples were analysed by PESA, H, C, N and O were not included in this analysis; however, preliminary results, obtained by applying PCA to the data sub-set relative to samples analysed by both techniques, showed that the presence of light elements does not change the statistical analysis results significantly.

Five factors were obtained, explaining 88% of the data variability. The analysis of the factor loadings, which are the correlation coefficients among the factors and the elemental concentrations, allowed an interpretation of these factors in terms of aerosol sources. We identified them as soil dust ('soil'), sea salt aerosol ('sea'), secondary sulfates ('sulfates') and two industrial sources ('industry 1' and 'industry 2'). Factor 'soil', characterized by crustal and soil-related elements, such as Al, Si, Ca, Ti and Fe, is connected to local soil re-suspension and to the aforementioned Saharan transport episodes. Factor 'sulfates' is characterized by S, whose gaseous precursor,  $\text{SO}_2$ , is mainly emitted from fossil fuel combustion processes, V and (to a less extent) Ni, which also are tracer elements for oil combustion. Factor 'sea', with high loadings of Na, Cl and Mg, is connected to the above quoted sea salt transport episodes. Factor 'industry 1' is characterized by Cu, Br, Ni, Cr and (to a less extent) K, whereas Zn and Pb are the elements with higher loadings in factor 'industry 2'.

Some of the elements with high loadings in the industrial sources, such as Cu, Zn and Cr, could also be connected with traffic; nevertheless, the analysis of the 2 h concentration data set excludes this possibility. In fact, the time trends of these elements did not show periodic daily variations with peaks during traffic rush hours, as we found in previous works.<sup>11–13</sup>

To determine the absolute weight and the profiles of the sources identified by PCA, and also the elemental source apportionments, we performed an absolute PCA (APCA), following the methods reported elsewhere.<sup>14,15</sup> The 'soil' and 'sulfates' sources turned out to give average contributions to the PM<sub>10</sub> mass of ~21 and ~11%, respectively, in good agreement with what we found by stoichiometric considerations, i.e. considering elements of crustal origin as oxides and S as ammonium sulfate (see 'Mass closure'). Furthermore, in the profile of the 'sulfates' source, S turned out to be ~23%, in very good agreement with the value expected from ammonium sulfate composition (24.2%). The industrial sources gave an average contribution of ~41% ('industry 1') and ~16% ('industry 2'). The marine aerosol source contribution was only a few percent, in agreement with the results of other studies of particulate matter in Florence.<sup>16</sup>

It is interesting that, although on average the anthropogenic contribution to PM<sub>10</sub> mass is dominant, if we look at the PM<sub>10</sub> source apportionment day by day, we found that during eight of the 21 days in which PM<sub>10</sub> mass was above the 50 µg m<sup>-3</sup> limit, the 'soil' source gave the main contribution (mainly due to Saharan dust episodes, as confirmed by HYSPLIT backward trajectory calculations).

## CONCLUSION

Using Teflon filters, both PIXE and PESA analyses are possible on the same samples, even if they must be performed separately. PIXE analyses on Teflon filters with standard Si(Li) detectors require a beam energy <3 MeV to avoid intolerable levels of background, whereas low energy beams are not suited for PESA, mainly owing to the worsening of the mass resolution. The coupling of the two techniques allows the 'mass closure', i.e. the measurement of the concentrations of all the elemental constituents of atmospheric aerosol.

A first aerosol characterization of the atmospheric aerosol in the area of Montelupo Fiorentino has been accomplished. The PM<sub>10</sub> concentration and composition were determined over a period spanning 9 months. C was found to be by far the main aerosol component, followed by N, O, Ca, Si, S, H and Fe. Fairly high As concentration levels were detected (with peaks up to 100 ng m<sup>-3</sup>) during the first sampling months, related to emissions from artistic glass manufacture.

The simultaneous sampling of PM<sub>10</sub>, PM<sub>2.5</sub> and PM<sub>1</sub> fractions allowed us to investigate the elemental size distributions. Soil-related elements were more abundant, as expected, in the coarse fraction, whereas anthropogenic

elements, such as As and S, were concentrated in the fine fraction.

During the campaign, a strong Saharan dust intrusion was identified and characterized thanks to the fractionating sampling and the multi-elemental feature of the PIXE and PESA techniques.

An APCA showed industrial sources to be, on average, the main contributors to PM<sub>10</sub> mass; however the weight of the 'soil' source (connected to local soil re-suspension and to long-range Saharan transport episodes) becomes dominant during some of the days in which the 50 µg m<sup>-3</sup> limit, set by EU Air Quality Directive, is exceeded. This investigation will be further extended after completing the PESA analysis of the remaining samples, thus allowing us to include light elements in the statistical analysis.

## Acknowledgment

The authors thank the Italian Ministry of Education, University and Research for financial support of this work in the frame of a wider research project (COFIN2001).

## REFERENCES

- Formenti P, Prati P, Zucchiatti A, Lucarelli F, Mandò PA. *Nucl. Instrum. Methods B* 1996; **113**: 359.
- Del Carmine P, Lucarelli F, Mandò PA, Moscheni G, Pecchioli A, MacArthur JD. *Nucl. Instrum. Methods B* 1990; **45**: 341.
- Boni C, Cereda E, Braga-Marcazzan GM, De Tomasi V. *Nucl. Instrum. Methods B* 1988; **35**: 80.
- Micklich BJ, Smith DL, Massey TN, Fink CL, Ingram D. *Nucl. Instrum. Methods A* 2003; **505**: 1.
- Maxwell JA, Teesdale WJ, Campbell JL. *Nucl. Instrum. Methods B* 1995; **95**: 407.
- Chiari M, Del Carmine P, Lucarelli F, Marcazzan G, Nava S, Papperetti L, Prati P, Valli G, Vecchi R, Zucchiatti A. *Nucl. Instrum. Methods B* 2004; **219–220**: 166.
- Draxler RR, Hess GD. *Aust. Meteorol. Mag.* 1998; **47**: 295.
- Viana M, Querol X, Alastuey A, Cuevas E, Rodriguez S. *Atmos. Environ.* 2002; **36**: 5861.
- Bonelli P, Braga-Marcazzan GM, Cereda E. *The Impact of Desert Dust Across the Mediterranean*. Kluwer: Dordrecht, 1996; 275.
- Chan YC, Simpson RW, McTainsh GH, Vowles PD, Cohen DD, Bailey GM. *Atmos. Environ.* 1997; **22**: 3773.
- Del Carmine P, Lucarelli F, Mandò PA, Valerio M, Prati P, Zucchiatti A. *Nucl. Instrum. Methods B* 1999; **150**: 450.
- Prati P, Zucchiatti A, Lucarelli F, Mandò PA. *Atmos. Environ.* 2000; **34**: 3149.
- D'Alessandro A, Lucarelli F, Mandò PA, Marcazzan G, Nava S, Prati P, Valli G, Vecchi R, Zucchiatti A. *J. Aerosol Sci.* 2003; **34**: 243.
- Swietlicki E, Puri S, Hansson HC. *Atmos. Environ.* 1996; **30**: 2795.
- Thurston GD, Spengler JD. *Atmos. Environ.* 1985; **19**: 9.
- Lucarelli F, Mandò PA, Nava S, Prati P, Zucchiatti A. *Air Waste Manage. Assoc. J.* 2004; **54**: 1372.